

## MIT Open Access Articles

*Development of a pointing, acquisition, and tracking system for a CubeSat optical communication module*

The MIT Faculty has made this article openly available. **Please share** how this access benefits you. Your story matters.

**Citation:** Tam Nguyen ; Kathleen Riesing ; Ryan Kingsbury and Kerri Cahoy " Development of a pointing, acquisition, and tracking system for a CubeSat optical communication module ", Proc. SPIE 9354, Free-Space Laser Communication and Atmospheric Propagation XXVII, 935400 (March 16, 2015)

**As Published:** <http://dx.doi.org/10.1117/12.2080591>

**Publisher:** SPIE

**Persistent URL:** <http://hdl.handle.net/1721.1/107999>

**Version:** Final published version: final published article, as it appeared in a journal, conference proceedings, or other formally published context

**Terms of Use:** Article is made available in accordance with the publisher's policy and may be subject to US copyright law. Please refer to the publisher's site for terms of use.



# Development of a pointing, acquisition, and tracking system for a CubeSat optical communication module

Tam Nguyen, Kathleen Riesing, Ryan Kingsbury, Kerri Cahoy

Massachusetts Institute of Technology, 77 Massachusetts Avenue, Cambridge, MA 02139

## ABSTRACT

Miniaturized satellites such as CubeSats continue to improve their capabilities to enable missions that can produce significant amounts of data. For most CubeSat missions, data must be downlinked during short low-earth orbit ground station passes, a task currently performed using traditional radio systems. Free-space optical communications take advantage of the high gain of a narrow optical beam to achieve better link efficiency, allowing more valuable data to be downlinked over the mission lifetime. We present the Nanosatellite Optical Downlink Experiment (NODE) design, capable of providing a typical 3U (30 x 10 x 10 cm) CubeSat with a comparatively high data-rate downlink. The NODE optical communication module is designed to fit within a 5 x 10 x 10 cm volume, weigh less than 1 kg, and consume no more than 10 W of power during active communication periods. Our design incorporates a fine-steering mechanism and beacon-tracking system to achieve a 10 Mbps link rate. We describe the system-level requirements and designs for key components, including a transmitter, a beacon tracking camera, and a fast-steering mirror. We present simulation results of the uplink beacon tracking and fine steering of the downlink beam, including the effects of atmospheric fading and on-orbit environmental disturbances to demonstrate the feasibility of this approach.

**Keywords:** laser communication, CubeSat, pointing, tracking, acquisition, beacon, fast-steering mirror

## 1. INTRODUCTION

Small satellites such as CubeSats are among the fastest growing classes of satellite in the last decade partly because of low cost components and availability of launch opportunities. Hundreds of CubeSats have been launched in the past decade, with a steep increase in number expected in the upcoming years.<sup>1</sup> CubeSat standards have strict size and weight requirements, where 1 CubeSat unit (1U) is 10 cm x 10 cm x 10 cm in volume and 1.33 kg in weight, and 3U CubeSats (10 cm x 10 cm x 30 cm, 4.0 kg) are common.<sup>2</sup> CubeSats were initially developed for educational purposes and as early technology demonstrations, but they have evolved fairly rapidly in capability. New advances in system-level design, improvements in three-axis control and onboard processing, and the desire to obtain near real-time, persistent observations mean that a significant amount of data will be produced.<sup>3,4</sup>

The amount of useful data successfully collected from a CubeSat mission is limited by low-rate RF downlinks. Most CubeSats are in LEO and have fairly short ground station access times (<10 min/pass). The platform constraints also restrict key RF performance parameters, gain (requires larger apertures) and power. While the RF mission downlink capability can also be improved by having a larger number of ground stations or a much larger ground station with higher gain, these options are expensive. RF systems also have a complicated licensing process and security concerns due to their relatively large beamwidths. There is a growing demand in the nanosatellite field for higher rate downlinks with less regulatory complexity and lower cost. With recent and anticipated improvements in CubeSat spacecraft pointing capabilities and some novel approaches to beam control presented here, laser communication technology has the potential to improve the communication bottleneck for CubeSats.

We present the pointing, acquisition and tracking system design of the Nanosatellite Optical Downlink Experiment (NODE) module, a laser communication downlink terminal for CubeSats from low-Earth orbit (LEO). The conservative NODE baseline design is capable of data rates of >10 Mbps (stretched goal of 50 Mbps), an improvement compared with most existing CubeSat RF systems (usually <1 Mbps).<sup>5</sup> NODE uses a two-stage pointing control mechanism to achieve pointing performance of  $\pm 0.09$  mrad  $3\text{-}\sigma$  without bias, sufficient for a 2.1 mrad downlink laser. The coarse stage relies on the host spacecraft body pointing capability and the fine

stage is driven by a miniature MEMS fast-steering mirror. Precise attitude sensing is accomplished by the use of a beacon system in addition to common CubeSat attitude sensors such as sun sensors, magnetometers, Earth horizon sensors. The handoff between coarse and fine control is dictated by the satellite body control capabilities under on-orbit disturbances. This approach is different from other CubeSat optical communication experiments under development, such as the Optical Communication and Sensor Demonstration (OCS-D), currently being developed at Aerospace Corporation, which relies only on the spacecraft body pointing mechanisms. The NODE module will fit within a 5 x 10 x 10 cm volume, weigh less than 1 kg, and consume no more than 10 W of power during active communication periods, in compliance with CubeSat size, weight, and power (SWaP) constraints.

## 2. MISSION OVERVIEW

In this section, we discuss the driving requirements, mission concept of operations, and the resulting pointing, acquisition, and tracking design for NODE.

### 2.1 Derivation of Requirements

The driving requirement of NODE is to provide an optical downlink that is competitive with existing RF systems. Based on surveys of existing CubeSat radios, NODE targets a data rate of 10-50 Mbps with comparable power consumption to existing RF solutions.<sup>5</sup> While the high-rate downlink and beacon uplink are optical, NODE also uses a low-rate RF uplink and downlink for high-level command and control and limited data downlink during any periods of optical link unavailability. The RF link is designed such that it can be supported with minimal resources in terms of licensing, ground systems, and power. As shown in Figure 1, an optical uplink beacon at 850 nm is utilized for acquisition and tracking, and an optical downlink beam at 1550 nm is used for high-rate data transmission.

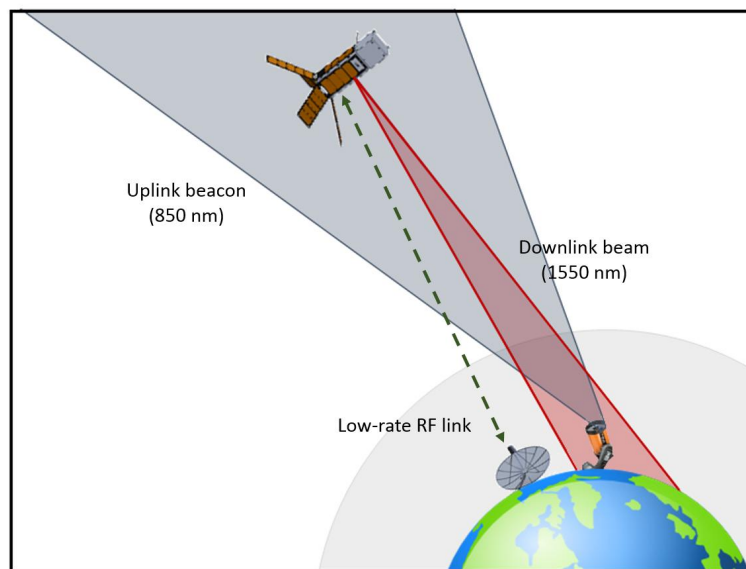


Figure 1: NODE mission architecture

The requirement for a 10 Mbps downlink rate and relatively small, inexpensive, and portable ground terminals determines the optical power that needs to be transmitted from NODE. Through a link budget analysis, a target beamwidth of 2.1 mrad was selected.<sup>6</sup> The targeted beamwidth then leads to the requirement for the pointing, acquisition, and tracking system to reduce pointing losses to acceptable levels. The flow of requirements is shown in Figure 2.

The NODE module is designed to be compatible with a typical 3-axis stabilized CubeSat. The current state-of-the-art in demonstrated CubeSat absolute pointing accuracy ranges from 1-5° RMS.<sup>3,7</sup> To achieve a 10-50

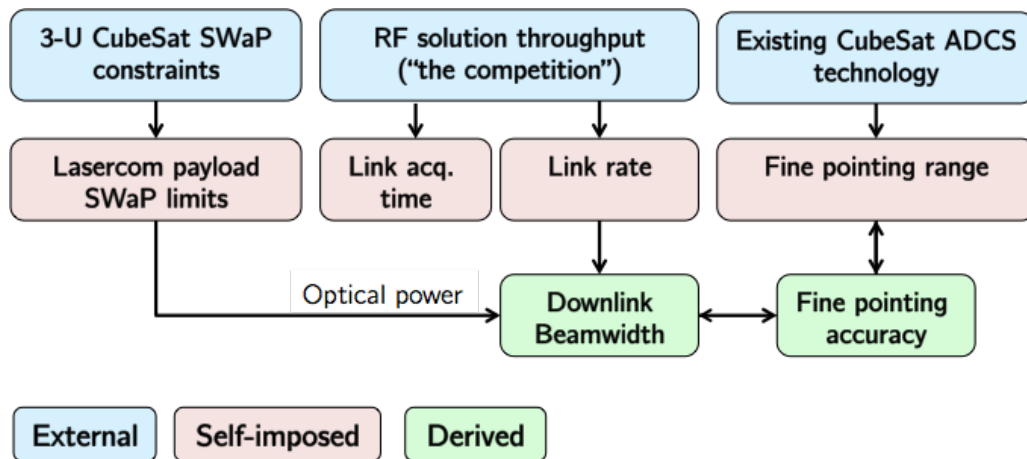


Figure 2: Derivation of requirements for NODE

Mbps link within the power constraints of a typical CubeSat, a finer pointing accuracy is required. Therefore, NODE takes a two-stage control approach in which the coarse body pointing is augmented with a fast-steering mirror (FSM) for fine control.

## 2.2 Concept of Operations

During a planned communications pass, the satellite uses its on-board propagated orbit to point towards the ground station and wait for an uplink beacon. The field-of-view of the beacon camera on the satellite is selected to cover the entirety of the uncertainty region so that no additional maneuvers are required to search for the ground station. Once the CubeSat beacon camera detects the signal from the ground station, it uses this information to improve the pointing accuracy to within the range of the fine stage. Finally, the FSM steers the transmit beam to the accuracy required for downlink.

The FSM is in a bistatic configuration, so there is no feedback on the position of the FSM. An on-orbit calibration procedure is necessary to ensure transmitter/receiver alignment. This calibration will utilize the low-rate RF link to communicate the received power measurements on the ground back up to the satellite. Using this feedback, the satellite can adjust its pointing until peak power is received on the ground.

## 3. SYSTEM DESIGN

The NODE spacecraft payload consists of two main subsystems: a downlink transmitter and an uplink beacon receiver. Due to size constraints, the payload uses a bistatic design, with separate downlink and uplink beacon paths. The physical layout of the payload is given in Figure 3. The transmitter design follows a Master Oscillator Power Amplifier (MOPA) architecture, where an Erbium Doped Fiber Amplifier (EDFA) is used in conjunction with a 1550 nm seed laser to provide a high peak-to-average power optical waveform. A fiber collimator forms the transmit beam which is subsequently directed by the fast steering mirror (FSM) in a "gimballed-flat" topology. The selected FSM is a MEMS tip/tilt mirror that meets the SWaP requirements as well as the steering range needed for coarse stage hand-off. The beacon receiver camera consists of a CMOS focal plane array with high sensitivity in the near-infrared (NIR) range to detect a 850 nm beacon transmitted from the ground station. The uplink beam image is processed with centroiding algorithms for fine attitude determination.

### 3.1 Attitude Determination Control System Stages

#### 3.1.1 Coarse Stage Design

The coarse stage of the pointing, acquisition, and tracking system consists of the CubeSat body pointing. The coarse pointing sensors and actuators are not contained within NODE, but rather the host CubeSat. NODE is agnostic to the choice of sensors and actuators in the host system, as long as the host is capable of meeting the

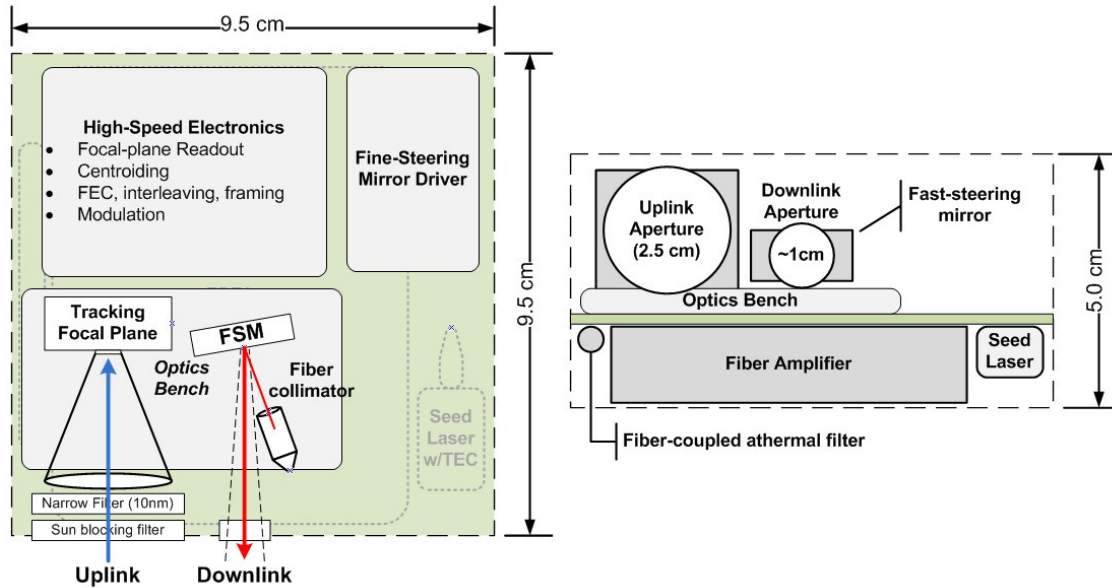


Figure 3: Physical layout of the NODE system<sup>6</sup>

requirements shown in Table 1. The host CubeSat must have sufficient orbit and attitude knowledge to initially point within  $3^\circ$  of the ground station. This requirement is based on the field-of-view of the beacon receiver. Once the beacon has been located, it provides very fine attitude knowledge, approximately  $30 \mu\text{rad}$ , and the CubeSat undergoes a transition to become actuation-limited. At this point, the host CubeSat must be capable of pointing to within  $1^\circ$  of accuracy to overlap with the range of the fine stage. NODE, which contains a FSM for fine steering, can then "dial in" the transmitter to the required accuracy for downlink.

Table 1: Host CubeSat requirements

Parameter	Requirement
Initial pointing accuracy	$\pm 3^\circ$
Actuation-limited pointing accuracy	$\pm 1^\circ$
Max. slew rate	up to $1.1^\circ/\text{s}$ (orbit dependent)

### 3.1.2 Fine Stage Design

Requirements for the accuracy of the fine stage are based on a detailed link budget analysis to size the beamwidth of NODE.<sup>6</sup> With a beamwidth of  $2.1 \text{ mrad}$ , the 3-pointing accuracy is set as a quarter of the beamwidth, or  $525 \mu\text{rad}$ . The pointing loss is thus limited to 3 dB in the worst case. Therefore, the key parameters of fine stage are a range of  $1^\circ$  to overlap with the CubeSat body pointing and a final accuracy of  $525 \mu\text{rad}$ , as summarized in Table 2.

Table 2: Node pointing requirements

Parameter	Requirement
Range	$\pm 1^\circ$
Pointing accuracy	$525 \mu\text{rad}$ ( $0.03^\circ$ )

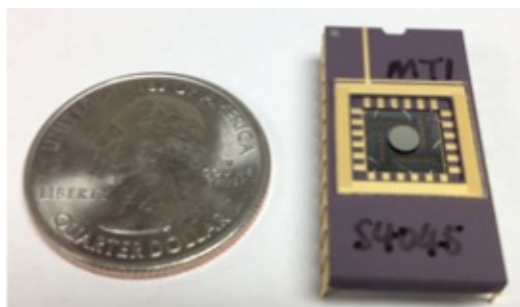


Figure 4: Fast steering mirror utilized in NODE from Mirrorcle Technologies, Inc.

A simple setup was developed to characterize the device, which is pictured in Figure 5.<sup>8</sup> A 650 nm red laser is directed through a focusing lens, which the FSM steers into a Si camera. From the geometry of the setup, the angle of the FSM can be determined. Since there is no feedback available on the devices position, it was necessary to characterize repeatability of the device to ensure it could meet performance requirements.

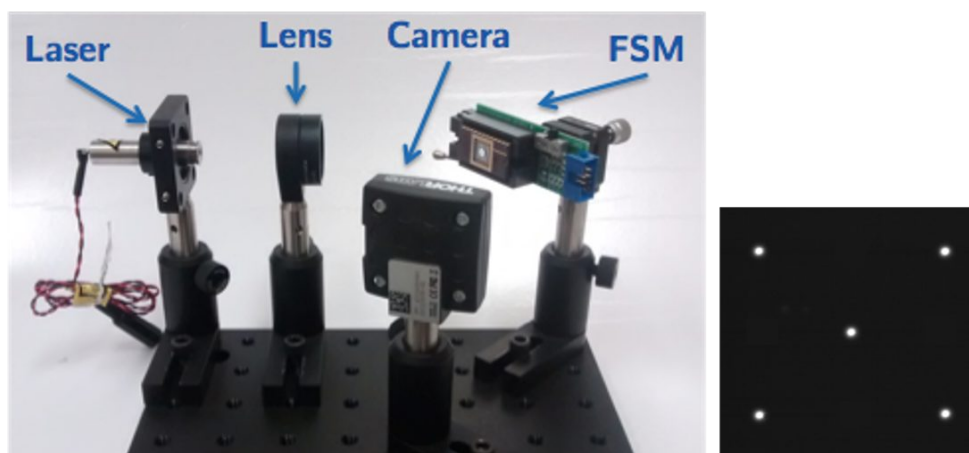


Figure 5: Experimental setup for FSM characterization (left)<sup>8</sup> and 5-sided die pattern used for repeatability analysis (right)

To test repeatability, the mirror was commanded to visit each of the points in a 5-sided die pattern covering its entire range. For each iteration, as shown in the focal plane in Figure 5, points were visited in a random order. Statistics on the position repeatability for a significant number of trials ( $N=500$ ) show that the RMS error of the device is  $12 \mu\text{rad}$ , well within the desired performance. Future testing will aim to ensure repeatability under varying thermal environments. Prior simulation analysis has shown that the staged setup remains well within the accuracy requirement.<sup>6</sup>

### 3.2 Beacon Camera Design

The beacon receiver camera consists of a CMOS focal plane array, a 1" aperture lens system, and two optical filters. The detector was chosen because of its high NIR sensitivity, resolution and low dark current and read noise properties. The lens system is an off-the-shelf product, providing a wide effective field-of-view ( $7^\circ$ ) that can sufficiently compensate for the satellites pointing capability with only coarse sensors. Two optical filters are used: a bandpass filter at 850 nm and a UV/VIS-cut filter to reduce heating caused by Sun radiation. A summary of the specifications of the uplink beacon camera can be found in Table 3. The current beacon camera prototype is shown in Figure 6. The system size is approximately 4 cm x 4 cm x 9.4 cm with a total weight of 160 g.

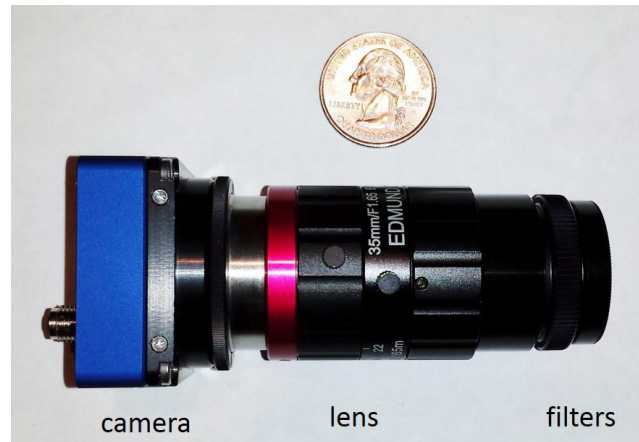


Figure 6: NODE beacon camera prototype

Table 3: Beacon camera parameters

Parameter	Value
Detector resolution	2592H x 1944V
Pixel's pitch	2.2 $\mu\text{m}$
Focal length	35 mm
Field of view	7°
850 nm band-pass filter bandwidth	10 nm
Long-pass filter cut-off frequency	700 nm

## 4. SIMULATION

### 4.1 Uplink beacon acquisition

The NODE satellite fine attitude sensing capability relies on the the acquisition and tracking of the uplink beacon. Since fading of the uplink beacon due to atmospheric turbulence is a major concern, especially with the high slew speed required to track the satellite in LEO (up to  $1^\circ/\text{s}$ ), detailed analysis and simulation was necessary to evaluate the performance of the beacon system.

Table 4 presents the beacon uplink budget with a 10 W transmitter, 5 mrad beamwidth when the satellite is at  $20^\circ$ , and  $90^\circ$  elevation angle, with estimates of optical and atmospheric absorption and scattering losses. Noise components in the simulation include shot noise from signal, background sky radiance, and the noise sources of the beacon camera detector. For the NODE design, background shot noise is the dominant source. Various background light conditions were analyzed including a worst case scenario consisting of sunlit clouds. The estimated spectral radiance in this condition at 850 nm is approximately  $180 \text{ W}/\text{m}^2/\text{sr}/\mu\text{m}$ .<sup>9</sup> The estimated integration time is selected to maximize dynamic range given the well capacity of the detector.

The atmospheric refractive index structure parameter ( $C_n^2$ ) profile for the mission can be estimated using the Hufnagel-Valley model. Since uplink beam will be slewing up to  $1^\circ/\text{s}$  to track the satellite in LEO, the slew rate becomes the dominant "wind-speed" parameter. This slew rate was incorporated in the Hufnagel-Valley model as additional wind speed through the Bufton wind model, leading to a more turbulent  $C_n^2$  profile than the standard HV5/7 profile, as seen in Figure 7. The scintillation index can be estimated using the strong-turbulence model.<sup>10</sup> The high scintillation index caused by a fast slew rate can be reduced by the use of multiple independent transmitters for spatial diversity. For a satellite at 400 km altitude, the scintillation index of the uplink channel with 4 independent transmitters is approximately 0.3. Signal power fluctuations about the mean



Table 4: Beacon link budget

Transmitter			
Transmit laser power	10		W
Uplink wavelength	850		nm
Beam divergence	5		mrad
Actual transmit power	4		W
Free-space/Atmospheric channel			
	20° elevation	90° elevation	
Range	984	400	km
Atmospheric absorption and scattering	-6	-5	dB
Receiver			
Receiver bandwidth	10	10	nm
Average power at detector	0.013	0.081	nW
Integration time	1.6	0.5	ms
Total photons received	7.3E+04	1.8E+05	photons
Noise level in ROI	7.0E+03	9.9E+03	photons
Optical S/N	10.1	12.5	dB

value from the above link budget can be estimated using a log-normal distribution with variance equal to the scintillation index.

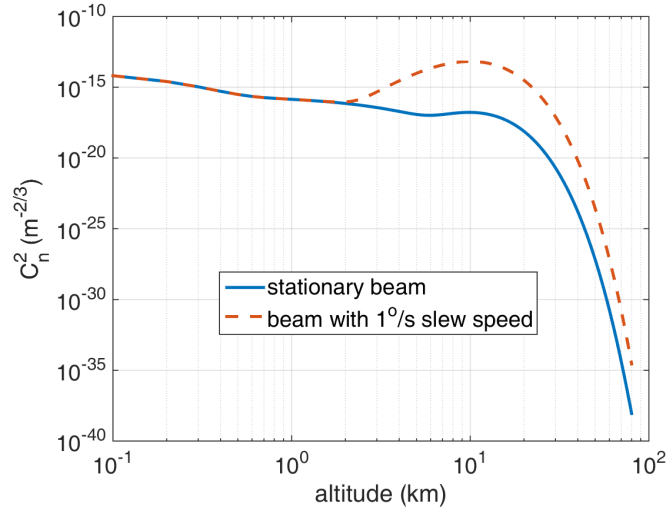


Figure 7:  $C_n^2$  profiles from Hufnagel-Valley model for a stationary beam and a beam slewing at  $1^\circ/\text{s}$

The fade probability and centroiding accuracy were found by running the simulation with scintillation statistics with a time series of expected beam motion at  $20^\circ$  elevation from a 400 km altitude orbit. A fade instance is defined as the case where the brightest pixel does not belong to the beacon image on the detector array. In this simulation, the scintillation time scale is assumed to be comparable to the detectors integration time.

The fade probability indicates the probability that the beacon is not found within the time it takes to read out a frame, which is approximately 0.15 s for a 5 Mpixel camera. Figure 8a shows the simulation results of fade probability at various transmitter power levels (5W, 7.5W, 10W). It can be seen that the fade probability can be reduced to about 2.3% given a 10 W transmit power, sufficient for acquisition and tracking given proper real-time estimation techniques.



The centroiding accuracy was found using center-of-mass centroiding of the beacon image on the detector. The accuracy result when not fading is shown in Figure 8b. The average centroiding accuracy is approximately 0.5 pixel, corresponding to a mean attitude accuracy of  $30\ \mu\text{rad}$ . This accuracy result is less than 1/10 of the pointing requirement of the fine stage, leaving margin for actuation limitations and errors.

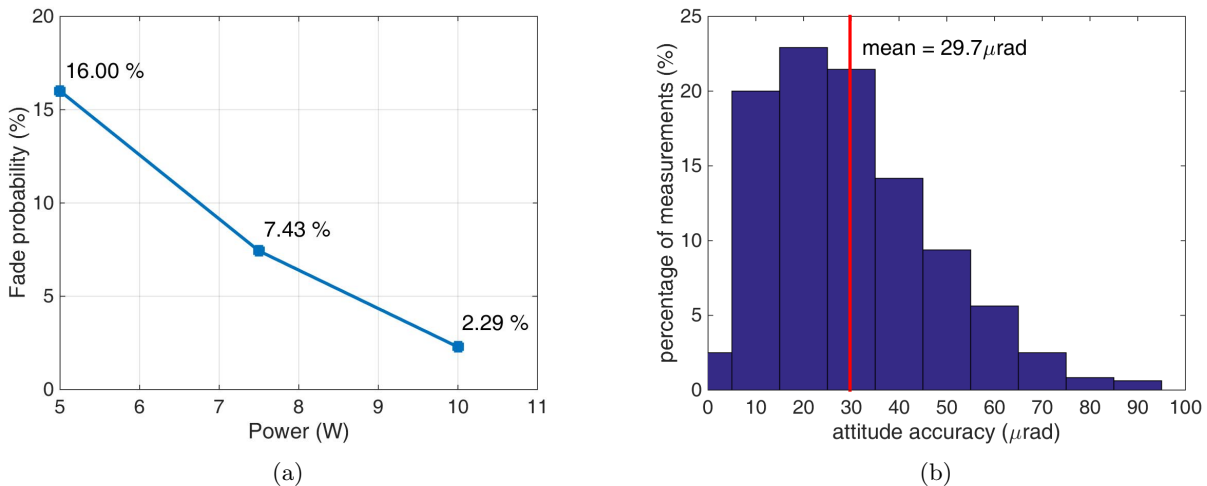


Figure 8: Beacon acquisition simulation results. (a) Fade probability with various transmit laser power levels (b) Pointing accuracy from centroiding

## 4.2 Control System Simulation

A simulation of the coarse and fine control stages was developed to ensure the design meets performance requirements.<sup>6</sup> While the coarse stage performance depends on the host CubeSat, parameters were based on recent CubeSat missions developed in the MIT Space Systems Lab.<sup>11,12</sup> Incorporating the results of the uplink beacon simulation described in the previous section, the accuracy of the detector is taken to be  $30\ \mu\text{rad}$  on average. The rate at which the FSM can be driven is limited by the beacon detector readout and processing. A readout rate of 10 Hz is sufficient to meet the requirement of  $525\ \mu\text{rad}$  accuracy, as shown in Figure 9. Once the beacon has been acquired, the CubeSat pointing performance is very dependent on the control authority of its reaction wheels. The CubeSat modeled in Figure 9 is very affected by torque quantization and is intended as a fairly low-performance actuator. Verifying that the fine stage can improve performance to within required accuracy (with a margin of 7 dB) for this scenario indicates that it can meet the pointing requirement for a typical CubeSat.

A limitation of this simulation is that it does not account for potential misalignment between the beacon detector and the FSM. Work is ongoing to assess methods of alignment and calibration using the low-rate RF link to detect and correct for any alignment biases. Furthermore, development of a full 6 degree-of-freedom simulation is underway to model momentum control and the effects of gyroscopic coupling on the system.

## 5. CONCLUSION

This paper describes the development of the NODE project currently being developed at the Space Systems Laboratory at MIT, with emphasis on the pointing, acquisition, and tracking system. The goal data rate is 10 Mbps (stretched goal of 50 Mbps), where high-accuracy pointing is achieved by the use of a two-stage control system. Preliminary analysis and simulation results were presented to demonstrate the capability of the system. The beacon system can provide an attitude knowledge accuracy of  $30\ \mu\text{rad}$  with 2.3% fading probability in each frame read-out. The combination of the coarse and fine stage control can achieve a pointing accuracy of  $\pm 90\ \mu\text{rad}$ , excluding consideration of pointing bias. This gives approximately 7dB of margin over the requirement of  $\pm 525\ \mu\text{rad}$ . In the worst case scenario, the pointing loss is maintained within 3dB.

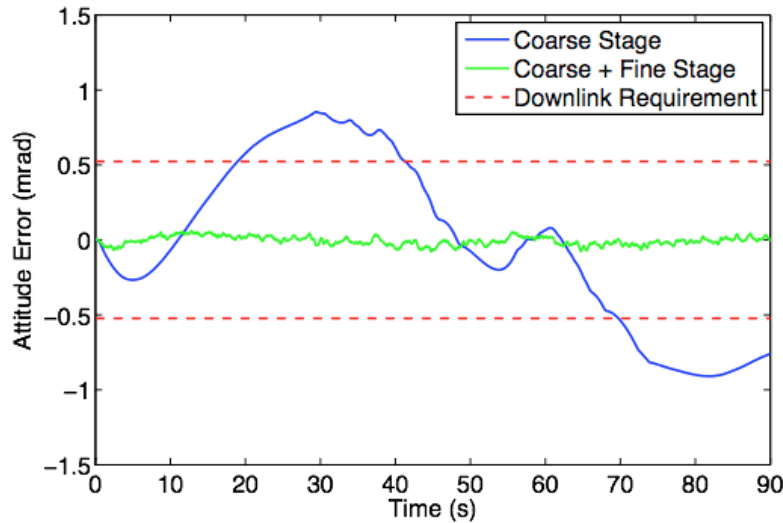


Figure 9: Simulation results for NODE tracking accuracy.

Next steps in the project include testing with hardware in the loop, system integration and algorithm development. Furthermore, initial simulation results show that a calibration procedure can eliminate initial pointing bias, and further calibration analysis is ongoing.

## REFERENCES

1. M. Swartwout, "The first one hundred cubesats: A statistical look," *Journal of Small Satellites* **2**, pp. 213–233, 2013.
2. "Cubesat design specification rev. 13," 2014.
3. A. Schwarzenberg-Czerny, W. Weiss, A. Moffat, R. Zee, and S. Rucinski, "The BRITE nano-satellite constellation mission," in *Proc. of 38th COSPAR Scientific Assembly*, 2010.
4. J. Hanson, J. Chartres, H. Sanchez, and K. Oyadomari, "The EDSN intersatellite communications architecture," in *Proc. of 28th AIAA/USU Conference on Small Satellites*, 2014.
5. B. Klofas and K. Leveque, "A survey of cubesat communications systems: 2009-2012," in *Proc. of CalPoly CubeSat Developers Workshop*, 2013.
6. R. Kingsbury, K. Cahoy, and K. Riesing, "Design of a free-space optical communication module for small satellites," in *Proc. of 28th AIAA/USU Conference on Small Satellites*, 2014.
7. J. Gangestad, B. Hardy, and D. Hinkley, "Operations, orbit determination, and formation control of the aerocube-4 cubesats," in *Proc. of 27th AIAA/USU Conference on Small Satellites*, 2013.
8. R. Kingsbury, T. Nguyen, K. Riesing, and K. Cahoy, "Fast-steering solutions for cubesat-scale optical communication," in *Proc. of International Conference on Space Optics*, 2014.
9. S. Lambert and W. Casey, *Laser Communications in Space*, Artech House Publishers, Boston, MA, 1995.
10. L. Andrews and R. Phillips, *Laser Beam Propagation through Random Media*, SPIE press, Bellingham, Washington, 2005 (second edition).
11. E. Wise, C. Pong, D. Miller, T. Nguyen, and K. Cahoy, "A dual-spinning, three-axis-stabilized cubesat for earth observations," in *AIAA Guidance, Navigation, and Control (GNC) Conference*, 2013.
12. C. Pong, *High-Precision Pointing and Attitude Estimation and Control Algorithms for Hardware-Constrained Spacecraft*. PhD thesis, Massachusetts Institute of Technology, 06 2014.